J. Biochem. 2013;153(2):209–220 doi:10.1093/jb/mvs142

JB THE JOURNAL OF BIOCHEMISTRY

iTRAQ-based quantitative proteomic analysis of submandibular glands from rats with STZ-induced hyperglycemia

Received July 26, 2012; accepted October 23, 2012; published online December 5, 2012

Renato M.P. Alves[1], Rui Vitorino[1], Ana I. Padrão[1], Daniel Moreira-Gonçalves[2], José A. Duarte[2], Rita M.P. Ferreira[1] and Francisco Amado[1,*]

[1]QOPNA, Department of Chemistry, University of Aveiro, 3810-193 Aveiro, Portugal; and [2]CIAFEL, Faculty of Sports, University of Porto, 4200-450 Porto, Portugal

*Francisco Amado, Escola Superior de Saúde da Universidade de Aveiro, Campus de Santiago, 3810-190 Aveiro, Portugal. Tel: +351-234-234-401-558, Fax: +351-234-401-597, email: famado@ua.pt

The impairment of salivary glands activity is often connected to the complaints of dry-mouth and subsequent degradation of the periodontium of diabetic patients. In this context, submandibular glands (SMGs) play a central role in saliva production and so the understanding of the molecular pathways affected is of paramount importance. Using a streptozotocin-induced hyperglycemia rat model and two different time points (2 and 4 months), we applied mass spectrometry-based proteomic techniques, validated with standard western blot analysis, to identify and quantify the effect of chronic hyperglycemia on the proteome of SMGs. We observed significant variations of proteins such as kallikreins, protein S100A6 or annexins. After 2 months of hyperglycemia, we observed an early phase response characterized by a significant increase of protein S100A6, linked to the inflammatory response, together with the impairment of metabolic and energy production processes. On the other hand, vesicular transport appeared to be favoured in such conditions. Interestingly, in a long-term response to hyperglycemia after 4 months of exposure, we observed a general attenuation of the variations. In conclusion, we present data that support the existence of an adaptation of the gland to long-term stress.

Keywords: diabetes mellitus/kallikrein/salivary glands/vesicular transport.

Abbreviations: iTRAQ, isobaric tags for relative and absolute quantitation; STZ, streptozotocin; SMG, submandibular gland.

Diabetes mellitus has assumed pandemic proportions in the developed and developing world. The World Health Organization projects that diabetes-related deaths will double within two decades, and the burdens of diabetes and diabetes-associated complications in the economy are reaching alarming levels (*1*, *2*). A better understanding of the pathophysiology of the disease, provided by the unravelling of the mechanisms involved, will provide an important aid in the prevention and treatment of diabetic patients, and subsequent relieve of the weight of this disease in health systems worldwide (*2*). It is now established a direct link between diabetes and oral pathologies, with diabetic patients exhibiting a higher prevalence of periodontal diseases (*3*). Xerostomia, associated with pathological thirst, is a common manifestation of diabetes. Its origin is often linked to impaired salivary gland activity, namely in the ability to synthesize and secrete saliva (*4*, *5*). Producing ~70% of unstimulated saliva, the submandibular glands (SMGs) play a major role in the maintenance of oral health and lubrication (*6*). Thus, knowing the mechanisms that lead to glandular impairment in diabetes mellitus is essential to try to attenuate this condition.

A common model to study the effect of Type 1 diabetes mellitus on salivary glands is the streptozotocin (STZ)-induced destruction of pancreatic beta-cells resulting in the loss of the ability to produce insulin and consequent hyperglycemia (*7*). Reports on the effects of STZ-induced diabetes have suggested ultrastructural changes in rat SMGs with less than 1 month exposure to hyperglycemia, namely the fusion of granules and the accumulation of lipid vacuoles, eventually leading to cellular degeneration and death (*8*). However, in an apparent contradiction, Anderson *et al*. (*9*) reported that glands retained relatively normal physiological responses with up to 6 months of exposure to hyperglycemia. The same group has later resolved this contradiction reporting that the structural changes were mainly confined to the granular ducts, whereas granular acini remained mostly unchanged after 3 months, and only started to show some profile changes at 6 months of exposure (*10*). Nonetheless, the biochemical events underlying such structural changes remain largely undisclosed and a proteomic analysis of salivary glands could help to explain the histological alterations reported and ultimately link them to the variations in saliva composition and oral health.

Despite the extensive reports on the salivary secretions proteome (*11*–*15*), to the best of our knowledge, the existing reports on protein analysis of salivary glands, in either control or disease situations, were focused on specific proteins such as antioxidant defense proteins (*16*, *17*), mucins (*18*), proline-rich proteins (*18*, *19*), epidermal growth factor (*20*) or kallikreins (*21*).

Thus, the purpose of our study was to disclose some of the biochemical pathways that are affected by chronic hyperglycemia in the SMG. Applying

© The Authors 2012. Published by Oxford University Press on behalf of the Japanese Biochemical Society. All rights reserved

Downloaded from http://jb.oxfordjournals.org/ at Pennsylvania State University on September 13, 2016

proteomic techniques to identify and quantify the differences in the proteome of an organelle membranes-enriched fraction from SMGs, we were able to identify an early phase response after 2 months of hyperglycemia, with pronounced variations of kallikreins and proteins involved in vesicular transport, followed by some signs of tissue adaptation at 4 months of chronic hyperglycemia, as the variations were not so pronounced.

Materials and Methods

Chemicals

All reagents were supplied by Sigma-Aldrich (St Louis, MO, USA) with the highest degree of purity available, unless otherwise stated. The isobaric tags for relative and absolute quantitation (iTRAQ) Reagent-8Plex kit was supplied by Applied Biosystems (Foster City, CA, USA). Primary antibodies rabbit polyclonal anti-GAPH (ab9485), rabbit polyclonal anti-alpha 1 Sodium Potassium ATPase antibody (ab74945) and rabbit monoclonal anti-S100 alpha 6 antibody (ab134149) were supplied by Abcam (Cambridge, UK) and rabbit polyclonal anti-annexin A2 antibody (NBP1-19810) was supplied by Novus Biologicals (Littleton, CO, USA).

Animals

Forty 6-week-old male Wistar rats (Charles River Laboratories, Barcelona, Spain) were divided into two groups. The first group (diabetic, $n=20$) received an intraperitoneal injection of STZ (60 mg/kg in citrate buffer, pH 4.5) to induce diabetes, while the second (control, $n=20$) received an injection with the vehicle alone. Animals were considered diabetic if blood glucose was >200 mg/dl 3 days after the injection. Weekly measurements of blood glucose were performed during the first month to ensure that the hyperglycemia state was maintained. Animals were housed at constant temperature (21–24°C) on a daily light schedule of 12 h light versus dark. Food and water were provided *ad libitum*. Diabetic animals presented clear signs of polydipsia and polyuria. After 2 and 4 months, 10 rats from each group were sacrificed by cervical dislocation, resulting in four different groups: 2-month diabetic (D2M), 2-month control (C2M), 4-month diabetic (D4M) and 4-month control (C4M). SMGs were excised, weighted and frozen at −80°C until further processing. All procedures were performed in accordance with the Guide for the Care and Use of Laboratory Animals and after approval of the local ethics committee.

Preparation of SMG membrane fractions

Membrane-enriched fractions were prepared according to Feinstein and Schramm (*22*). In brief, both SMGs of two animals from each group ($n=2$) were homogenized in sucrose medium (0.25 M sucrose, 1 mM EDTA and pH 7.5) in a loose glass-Teflon homogenizer for 2 min at 700 rpm. The homogenate was centrifuged for 5 min at 250 × *g*, 4°C. The resulting supernatant was centrifuged for 10 min at 1,000 x *g* to obtain a pellet enriched in secretory granules and organelle membranes, which was resuspended in sucrose medium to a final concentration of 2–10 mg protein/ml. Protein concentration was estimated using the RC–DC method (Bio-Rad), according to the manufacturer's instructions.

Protein digestion and iTRAQ labelling

An in-solution digestion was performed for iTRAQ labelling. Briefly, 100 µg of protein was used for digestion which was performed according to the protocol provided by the manufacturer (Applied Biosystems). Briefly, samples were mixed with triethyl ammonium bicarbonate buffer (TEAB) (1 M and pH 8.5) and RapiGest (Waters) to a final concentration of 0.5 M and 0.1%, respectively. Samples were then reduced with 5 mM tris(2-carboxyethyl) phosphine for 1 h at 37°C and alkylated with 10 mM *S*-methyl methanethiosulfonate for 10 min at room temperature. Two micrograms of trypsin was added to each sample and the digestion was performed for 18 h at 37°C. Samples were dried in a SpeedVac (Thermo Savant).

Digested sample peptides were subsequently labelled with the iTRAQ reagents (8-plex) following the protocol provided by the manufacturer (Applied Biosystems). In brief, peptides were reconstituted in 70% ethanol/30% TEAB 500 mM, added to each label and incubated for 2 h at room temperature. The reaction was stopped by adding water and the labelled digests corresponding to each of the four 8-plex experiments were combined and dried using SpeedVac.

Protein identification and iTRAQ quantification by 2D-LC-MS/MS

Labelled peptides were separated by a multidimensional LC approach based on a first dimension with high pH reverse phase (as previously described (*23*)) and a second dimension with the acidic reverse-phase system. Sample loading was performed at 200 µl/min with buffers (A) 72 mM TEAB, 52 mM acetic acid in H_2O, pH 10 and (B) 72 mM TEAB, 52 mM acetic acid in acetonitrile (ACN), pH 10 (98% A:2% B). After 5 min of sample loading and washing, peptide fractionation was performed with linear gradient to 50% B over 35 min followed by a 100% B step. Sixteen fractions were collected, evaporated and resuspended in 2% ACN, 0.1% trifluoroacetic acid (TFA). Collected fractions were separated as previously described (*24*). Briefly, peptides loaded onto a C18 pre-column (5 µm particle size, 5 mm; Dionex) connected to an RP column PepMap100 C18 (150 mm × 75 µm i.d., 3 µm particle size). The flow rate was set at 300 nl/min. The mobile phases A and B were 2% ACN, 0.1% TFA in water and 95% ACN, 0.045% TFA, respectively. The gradient was started at 10 min and ramped to 60% B till 50 min and 100% B at 55 min and retained at 100% B till 65 min. The column was equilibrated with solvent A for 20 min before the next sample was injected. The separation was monitored at 214 nm using a UV detector (Dionex/LC Packings, Sunnyvale, CA, USA) equipped with a 3-nl flow cell. Using the micro-collector Probot (Dionex/LC Packings) and, after a lag time of 5 min, peptides eluting from the capillary column were mixed with a continuous flow of α-CHCA matrix solution (270 nl/min, 2 mg/ml in 70% ACN/0.3% TFA and internal standard Glu-Fib at 15 fmol) were directly deposited onto the LC-MALDI plates at 12 s intervals for each spot (150 nl/fraction). For every separation run, 208 fractions in total were collected.

The spectra were processed and analysed by the ProteinPilot software (v4.0 AB Sciex, USA), which uses paragon algorithm for protein/peptide identification based on MS/MS data against the SwissProt protein database (release date 01012011, all taxonomic categories). Default search parameters were used: trypsin as the digestion enzyme, methylthio on cysteine residue as fixed modification, iTRAQ 8Plex, biological modification with emphasis on phosphorylation and urea denaturation as the variable modification setting. Mass tolerances for precursor and fragments were default values for ProteinPilot®. Cut-off score value for accepting protein identification for ProteinPilot® was a ProteoScore of 1.3 (95% confidence). Data were normalized for loading error by bias correction, which is an algorithm in ProteinPilot that corrects for unequal mixing when combining the labelled samples of one experiment. It does so by calculating the median protein ratio for all proteins reported in each sample, adjusted to unity and assigning an autobias factor to it. The variation ratios were calculated individually against each of the individuals in the C2M group.

To ensure valid and statistically significant quantification, some exclusion criteria were developed and sequentially applied to the results obtained from the ProteinPilot software, selecting only the proteins that met the following conditions: (i) proteins were identified in all individuals, (ii) proteins could not present a variation >25% within the C2M, to eliminate individual variability; (iii) proteins presented at least two ratios with a *P*-value <0.05 and (iv) the standard deviation from the ratios selected was <30% of their average. Nevertheless, the quantification results were reviewed manually for all proteins found to be differentially expressed (iTRAQ ratio >1.25 or <0.75 according to (*25*)).

Western blot

Approximately 20 µg of protein from each fraction was electrophoresed on a 12.5% SDS–PAGE as described by Laemmli (*26*) and then blotted onto a nitrocellulose membrane (Millipore, Billerica, MA, USA). Nonspecific binding was blocked with 5% w/v dry non-fat milk in TBS-T (100 mM Tris, 1.5 mM NaCl, pH 8.0 and 0.05% Tween-20), followed by 3 h incubation with primary antibody (anti-GAPDH, anti-alpha 1 sodium potassium ATPase, anti-S100 alpha 6 and anti-annexin A2) diluted 1:1,000 in 5% w/v dry

Downloaded from http://jb.oxfordjournals.org/ at Pennsylvania State University on September 13, 2016

non-fat milk in TBS-T, washed and incubated with horseradish peroxidase-conjugated anti-rabbit IgG secondary antibodies diluted 1:5,000 in 5% w/v dry non-fat milk in TBS-T, at room temperature. Immunoreactive bands were detected by enhanced chemiluminescence ECL (GE Healthcare, Buckinghamshire, UK) on X-ray films (Hyperfilm ECL, GE Healthcare) and digital images were obtained using a Molecular Imager Gel Doc XR system (Bio-Rad, Hercules, CA, USA) and analysed with QuantityOne Software (v 4.6.3, Bio-Rad). Results are presented as mean ± SD for each experimental group of at least three independent experiments with $n = 2$.

Statistical analysis

All statistical tests were performed using GraphPad Prism v5.00 (GraphPad Software, Inc.). General data from the animals involved in the study (weight, glycemia, HbA_{1c} and gland weight) were analysed using a two-way ANOVA with Bonferroni's post-tests to compare groups. Western blot data were analysed using one-way ANOVA followed by Dunnett's multiple comparison test to compare each group to C2M group. A P-value <0.05 was considered significant.

Results

The animals used in this work developed a hyperglycemic state within 2 days of the injection with STZ (Table I). It was observed a significant difference in body weight, with a higher increase in controls. Other classical symptoms of diabetes, such as polydipsia and polyuria, were also observed throughout the experimental period.

Protein identification in SMG fractions by 2D-LC-MS/MS

A total of 462 distinct proteins were identified by 2D-LC-MALDI-TOF/TOF mass spectrometry (Supplementary Table S1). To obtain a global view of the protein classes represented in our fractions enriched in organelle membranes, we have submitted the list of proteins identified to the 'Compare gene lists' tool in the PANTHER website (www.pantherdb.org), which retrieved a classification in protein classes and if the percentage of genes in each category would be lower or greater than expected, by comparing the list submitted with a list of all the *Rattus norvegicus* genes. The major protein classes with more gene hits were nucleic acid binding, oxidoreductase, cytoskeleton protein and transfer/carrier protein (Supplementary Table S2). However, to obtain a more physiologically relevant insight, we performed a similar analysis that retrieved the classification in GO biological processes. Some of the over-represented GO biological processes were the metabolic process, with the lowest P-value, as well as other processes that may be associated to intra-cellular vesicular transport, such as protein transport, cellular component organization, vesicle-mediated transport and endocytosis (Table II). A closer analysis on the proteins included in these processes reveals the presence of two clathrin subunits, five annexins (from a total of only seven entries in Uniprot), six ras-related proteins and four coatomer subunits, clearly indicating an enrichment of membranous structures such as secretory granules. Also, from a total of nine entries in the Uniprot database, we have identified eight glandular kallikreins, all of which with a high number of peptides above the threshold of 95% and a high degree of coverage (Supplementary Table S1).

iTRAQ quantitative analysis of proteome variations with hyperglycemia

To disclose how hyperglycemia affects protein expression, we have applied iTRAQ quantification to the fractions obtained from the SMG. As can be depicted from Fig. 1, the proteins that passed the exclusion criteria present a high correlation when we compared the ratios of each individual versus each of the controls, ensuring that only proteins with low individual variability were selected. Also, the time-matched control group (C4M) presented almost all of the proteins below the limits established to consider a protein up- or down-regulated (Fig. 1C).

A total 107 proteins passed the exclusion criteria in the D2M group. From these, 31 were considered up-regulated, 67 were down-regulated and 9 proteins presented no variation versus control. Within the D4M group, 48 proteins passed the exclusion criteria, 10 of which were up-regulated, 28 presented no variation and 10 other were down-regulated versus C2M (Table III). Regarding the C4M group, 31 proteins passed the exclusion criteria and only three of these presented variation versus C2M (two were up-regulated and one was down-regulated). iTRAQ quantification results were validated by western blot analysis of selected proteins, namely GAPDH, alpha 1 sodium potassium ATPase, annexin A2 and protein S100A6 (Fig. 2).

The lists of proteins selected for each of the treated groups were then submitted to the PANTHER database for a broader view of the GO biological processes altered with hyperglycemia. Table IV summarizes the distribution of the genes corresponding to those proteins by GO Biological Process. After 2 months of hyperglycemia, >50% of the identified proteins

Table I. Average values of weight, glycemia, HbA1c and SMG weight from the animals involved in the experimental protocol.

Group	C2M	D2M	C4M	D4M
Weight (g)	394.5 ± 32.4	233.7 ± 33.2***	437.1 ± 58.4	251.0 ± 43.1***
Glycemia (mg/dl)	71.0 ± 12.2	–[a]	66.3 ± 14.9	–[a]
HbA1c (%)	5.7 ± 0.6	8.4 ± 0.3***	3.9 ± 0.8	6.3 ± 1.1***
SMG weight (g)	0.351 ± 0.014	0.218 ± 0.018***	0.319 ± 0.014	0.256 ± 0.034**
Protein recovered in fractions (mg protein/g tissue)	14.14 ± 1.40	1.35 ± 0.51***	14.89 ± 3.32	5.25 ± 2.23***

Data are presented as mean ± SD. [a]The glycemia values in STZ-treated rats were above the detection limit of the device used for the readings (>600 mg/dl). **$P < 0.01$; ***$P < 0.001$.

Downloaded from http://jb.oxfordjournals.org/ at Pennsylvania State University on September 13, 2016

Table II. Classification of the proteins identified by biological process.

Biological process	Number of gene hits			Over-/under-representation in the list of identified proteins	*P*-value
	Rattus norvegicus—Reference list (27,758)	List of identified proteins (456)	Expected		
Apoptosis	815	7	13.39	–	4.18E–02
Negative regulation of apoptosis	179	0	2.94	–	5.23E–02
Cell adhesion	962	8	15.8	–	2.27E–02
Cell–cell adhesion	484	3	7.95	–	4.25E–02
Cell communication	4,249	45	69.8	–	4.44E–04
Cell–cell signaling	869	6	14.28	–	1.11E–02
Signal transduction	4,065	43	66.78	–	5.90E–04
Cell surface receptor linked signal transduction	2,030	7	33.35	–	1.67E–08
G-protein coupled receptor protein signalling pathway	1,051	4	17.27	–	1.23E–04
Cytokine-mediated signalling pathway	272	0	4.47	–	1.12E–02
Transmembrane receptor protein tyrosine kinase signalling pathway	287	1	4.71	–	5.04E–02
Intracellular signalling cascade					
MAPKKK cascade	285	1	4.68	–	5.18E–02
Cell cycle	1,326	39	21.78	+	3.94E–04
Cellular component organization	1,215	50	19.96	+	4.12E–09
Cellular process					
Cell motion	469	18	7.7	+	9.48E–04
Chromosome segregation	153	6	2.51	+	4.25E–02
Cytokinesis	105	5	1.72	+	3.09E–02
Developmental process	2,381	57	39.11	+	2.86E–03
Anatomical structure morphogenesis	846	41	13.9	+	1.29E–09
Cellular component morphogenesis	846	41	13.9	+	1.29E–09
Embryonic development	181	0	2.97	–	5.06E–02
Pattern specification process	211	0	3.47	–	3.08E–02
System development					
Muscle organ development	192	9	3.15	+	5.05E–03
Generation of precursor metabolites and energy	401	41	6.59	+	4.82E–20
Oxidative phosphorylation	127	15	2.09	+	5.66E–09
Respiratory electron transport chain	376	29	6.18	+	1.43E–11
Tricarboxylic acid cycle	28	13	0.46	+	3.68E–15
Homeostatic process	87	6	1.43	+	3.47E–03
Cellular calcium ion homeostasis	45	6	0.74	+	1.18E–04
Immune system process					
Immune response	697	1	11.45	–	1.17E–04
B cell-mediated immunity	277	0	4.55	–	1.03E–02
Metabolic process	9,400	278	154.42	+	3.37E–32
Coenzyme metabolic process	90	10	1.48	+	3.36E–06
Nitrogen compound metabolic process	22	2	0.36	+	5.15E–02
Oxygen and reactive oxygen species metabolic process	51	7	0.84	+	2.68E–05
Primary metabolic process	8,928	252	146.67	+	2.68E–24
Carbohydrate metabolic process	784	46	12.88	+	2.08E–13
Monosaccharide metabolic process	232	20	3.81	+	3.51E–09
Gluconeogenesis	35	4	0.57	+	2.86E–03
Glycolysis	143	13	2.35	+	1.09E–06
Pentose-phosphate shunt	9	2	0.15	+	9.89E–03
Cellular amino acid and derivative metabolic process	297	15	4.88	+	1.57E–04
Cellular amino acid metabolic process	297	15	4.88	+	1.57E–04
Cellular amino acid biosynthetic process	82	6	1.35	+	2.60E–03
Cellular amino acid catabolic process	66	6	1.08	+	8.80E–04
Lipid metabolic process					
Fatty acid metabolic process	273	16	4.48	+	1.70E–05
Fatty acid beta-oxidation	26	6	0.43	+	5.69E–06
Phospholipid metabolic process	235	0	3.86	–	2.07E–02
Nucleobase, nucleoside, nucleotide and nucleic acid metabolic process					
DNA metabolic process					
DNA repair	200	0	3.29	–	3.70E–02
Purine base metabolic process	122	6	2	+	1.65E–02
Transcription	2,101	8	34.51	–	2.89E–08
Transcription from RNA polymerase II promoter	2,059	8	33.82	–	5.14E–08
Regulation of transcription from RNA polymerase II promoter	1,581	3	25.97	–	9.41E–09
Protein metabolic process	3,897	140	64.02	+	6.30E–20
Protein complex assembly	102	10	1.68	+	9.89E–06
Protein folding	253	19	4.16	+	7.30E–08

(continued)

Downloaded from http://jb.oxfordjournals.org/ at Pennsylvania State University on September 13, 2016

Table II. Continued

Biological process	Number of gene hits: *Rattus norvegicus*—Reference list (27,758)	List of identified proteins (456)	Expected	Over-/under-representation in the list of identified proteins	*P*-value
Protein modification process					
Protein amino acid phosphorylation	804	1	13.21	–	2.21E−05
Translation	957	76	15.72	+	1.18E−29
tRNA aminoacylation for protein translation	49	6	0.8	+	1.86E−04
Sulphur metabolic process	123	5	2.02	+	5.41E−02
Vitamin metabolic process	46	4	0.76	+	7.42E−03
Vitamin biosynthetic process	23	3	0.38	+	6.76E−03
Reproduction	391	2	6.42	–	4.45E−02
Response to stimulus					
Cellular defense response	374	0	6.14	–	2.06E−03
Response to stress	304	13	4.99	+	1.87E−03
Response to toxin	116	7	1.91	+	3.42E−03
System process					
Muscle contraction	355	13	5.83	+	6.72E−03
Neurological system process	1,480	10	24.31	–	7.02E−04
Sensory perception	557	2	9.15	–	5.21E−03
Visual perception	286	1	4.7	–	5.11E−02
Transport	2,647	93	43.48	+	2.21E−12
Protein transport	1,344	64	22.08	+	4.01E−14
Intracellular protein transport	1,344	64	22.08	+	4.01E−14
Protein targeting	162	6	2.66	+	5.31E−02
Vesicle-mediated transport	848	38	13.93	+	4.05E−08
Endocytosis	367	19	6.03	+	1.57E−05
Receptor-mediated endocytosis	141	8	2.32	+	2.62E−03
Exocytosis	273	13	4.48	+	7.25E−04
Unclassified	1,1957	41	196.43	–	1.58E−58

This table lists the GO biological processes enriched in the fractions analysed, with a *P*-value <0.05 according to the PANTHER database (www.pantherdb.org).

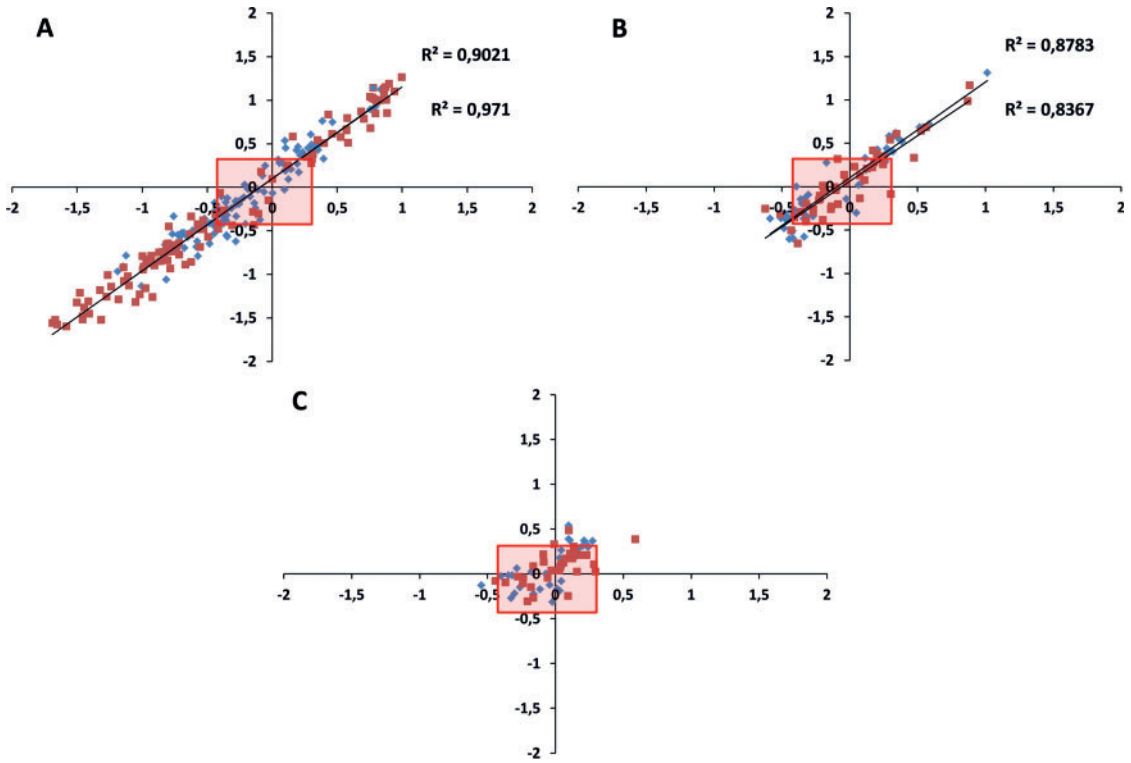

Fig. 1 Comparison of the protein variation ratios obtained for each animal in groups D2M (A), D4M (B) and C4M (C) versus each one of the control animals (*x*- and *y*-axis, respectively) from the C2M group. Filled squares and filled diamonds represent each one of the animals analysed in every group; each dot corresponds to a single protein, where the variation ratio versus each of the two animals of the C2M group can be read in the *x*- and *y*-axis, respectively. The shaded area in the centre delimits the area where it was considered that no variation occurred. It is observable a high correlation of the values for both animals in D2M (A) and D4M (B) groups, while almost all of the proteins in the C4M (C) group presented no significant variation.

Downloaded from http://jb.oxfordjournals.org/ at Pennsylvania State University on September 13, 2016

Table III. Protein abundance ratios determined by iTRAQ quantification when compared with the C2M group.

Total	% Cov	Accession #		Name	Peptides (95%)	D2M	C4M	D4M
7.18	49.4	P68255	1433T_RAT	14-3-3 protein theta	6	1.618 ± 0.238		
19.92	52.1	P00507	AATM_RAT	Aspartate aminotransferase, mitochondrial	10	0.746 ± 0.072		
11.89	83.9	P11030	ACBP_RAT	Acyl-CoA-binding protein	9	1.466 ± 0.039		
24.27	43.1	Q9ER34	ACON_RAT	Aconitate hydratase, mitochondrial	13	0.74 ± 0.089		0.833 ± 0.039
74.6	89.9	P63259	ACTG_RAT	Actin, cytoplasmic 2	65			0.782 ± 0.024
27.03	67.1	Q09073	ADT2_RAT	ADP/ATP translocase 2	15	0.477 ± 0.153		
9.9	33.2	P07150	ANXA1_RAT	Annexin A1	9	1.473 ± 0.123	1.198 ± 0.065	1.246 ± 0.056
13.63	33.3	Q07936	ANXA2_RAT	Annexin A2	7	1.868 ± 0.113	1.176 ± 0.014	1.435 ± 0.105
14.74	42	P55260	ANXA4_RAT	Annexin A4	6	1.42 ± 0.192		1.229 ± 0.034
24.52	40.9	P48037	ANXA6_RAT	Annexin A6	14			1.204 ± 0.013
4.37	25.8	Q4V7C7	ARP3_RAT	Actin-related protein 3	2	2.031 ± 0.159		
59.89	57.2	P06685	AT1A1_RAT	Sodium/potassium-transporting ATPase subunit alpha-1	44	1.744 ± 0.522	1.102 ± 0.295	1.351 ± 0.146
28.16	57.2	P07340	AT1B1_RAT	Sodium/potassium-transporting ATPase subunit beta-1	16	1.797 ± 0.522	1.198 ± 0.14	1.378 ± 0.178
11.95	37.1	P18596	AT2A3_RAT	Sarcoplasmic/endoplasmic reticulum calcium ATPase 3	6	1.049 ± 0.45		
8.7	32.8	P19511	AT5F1_RAT	ATP synthase subunit b, mitochondrial	3	0.607 ± 0.047		1.056 ± 0.347
8.45	54	P31399	ATP5H_RAT	ATP synthase subunit d, mitochondrial	4	0.535 ± 0.002		
9.23	70.4	P29419	ATP5I_RAT	ATP synthase subunit e, mitochondrial	7	0.67 ± 0.109	1.213 ± 0.051	0.755 ± 0.035
13.58	75.9	P21571	ATP5J_RAT	ATP synthase-coupling factor 6, mitochondrial	8	0.54 ± 0.031		
38.1	72	P15999	ATPA_RAT	ATP synthase subunit alpha, mitochondrial	30	0.515 ± 0.163		0.792 ± 0.042
51.42	81.1	P10719	ATPB_RAT	ATP synthase subunit beta, mitochondrial	36	0.535 ± 0.137		0.794 ± 0.066
10	73.2	P35434	ATPD_RAT	ATP synthase subunit delta, mitochondrial	6	0.427 ± 0.167		
7.42	57.3	Q06647	ATPO_RAT	ATP synthase subunit O, mitochondrial	6	0.555 ± 0.181		0.705 ± 0.064
17.31	60.4	P27139	CAH2_RAT	Carbonic anhydrase 2	9			1.52 ± 0.073
21.74	87.3	P62161	CALM_RAT	Calmodulin	13	2.023 ± 0.362		1.4 ± 0.19
43.99	86.1	P18418	CALR_RAT	Calreticulin	27		0.815 ± 0.016	
10.87	26.4	P35565	CALX_RAT	Calnexin	5	0.536 ± 0.037		
19.02	42.1	P63039	CH60_RAT	60 kDa heat shock protein, mitochondrial	10	0.773 ± 0.049		
10.42	26.4	Q8VHF5	CISY_RAT	Citrate synthase, mitochondrial	6	0.536 ± 0.014		
2.79	20.2	P08081	CLCA_RAT	Clathrin light chain A	4	1.872 ± 0.293		
7.46	43.2	P10888	COX41_RAT	Cytochrome c oxidase subunit 4 isoform 1, mitochondrial	6	0.535 ± 0.015		0.776 ± 0.034
11.24	45.9	P11240	COX5A_RAT	Cytochrome c oxidase subunit 5A, mitochondrial	11	0.447 ± 0.124		0.72 ± 0.077
12.13	54.3	P12075	COX5B_RAT	Cytochrome c oxidase subunit 5B, mitochondrial	8	0.613 ± 0.077		1.025 ± 0.343
8.09	72.1	P10818	CX6A1_RAT	Cytochrome c oxidase subunit 6A1, mitochondrial	6	0.464 ± 0.016		
13.35	55.2	Q7M0E3	DEST_RAT	Destrin	6	1.646 ± 0.06		
12.58	36	P10860	DHE3_RAT	Glutamate dehydrogenase 1, mitochondrial	6	0.563 ± 0.001		
10.35	22.1	Q920L2	DHSA_RAT	Succinate dehydrogenase [ubiquinone] flavoprotein subunit, mitochondrial	8	0.501 ± 0.109		0.74 ± 0.051
5.95	22.3	P21913	DHSB_RAT	Succinate dehydrogenase [ubiquinone] iron-sulfur subunit, mitochondrial	3	0.456 ± 0.058		
11.6	21.4	Q6P6R2	DLDH_RAT	Dihydrolipoyl dehydrogenase, mitochondrial	6	0.593 ± 0.033		
2.21	8.9	Q9R0T3	DNJC3_RAT	DnaJ homolog subfamily C member 3	2	0.606 ± 0.095		
24.01	40	Q64428	ECHA_RAT	Trifunctional enzyme subunit alpha, mitochondrial	16	0.635 ± 0.142		
4.4	18.3	Q60587	ECHB_RAT	Trifunctional enzyme subunit beta, mitochondrial	4	0.485 ± 0.033		

(continued)

Downloaded from http://jb.oxfordjournals.org/ at Pennsylvania State University on September 13, 2016

Table III. Continued

Total	% Cov	Accession #		Name	Peptides (95%)	D2M	C4M	D4M
6.41	37.9	P14604	ECHM_RAT	Enoyl-CoA hydratase, mitochondrial	3	0.645 ± 0.032		0.719 ± 0.035
18.74	60.2	P62630	EF1A1_RAT	Elongation factor 1-alpha 1	10		1.053 ± 0.248	1.022 ± 0.298
12	19.5	P85834	EFTU_RAT	Elongation factor Tu, mitochondrial	7	0.625 ± 0.023		
12.18	22.8	Q1JU68	EIF3A_RAT	Eukaryotic translation initiation factor 3 subunit A	7	0.732 ± 0.025	0.814 ± 0.022	0.767 ± 0.019
30.88	65.9	P04764	ENOA_RAT	Alpha-enolase	18	1.54 ± 0.265	1.148 ± 0.013	1.285 ± 0.052
30.4	45.5	Q66HD0	ENPL_RAT	Endoplasmin	16		0.782 ± 0.009	
11.36	52	P04797	G3P_RAT	Glyceraldehyde-3-phosphate dehydrogenase	7	1.863 ± 0.167		1.25 ± 0.135
8.19	21.1	P50399	GDIB_RAT	Rab GDP dissociation inhibitor beta	6	1.826 ± 0.025		
5.07	24.1	P09606	GLNA_RAT	Glutamine synthetase	3	1.771 ± 0.118		1.739 ± 0.211
17.33	37.7	P48721	GRP75_RAT	Stress-70 protein, mitochondrial	10	0.686 ± 0.112		
35.34	63.9	P06761	GRP78_RAT	78 kDa glucose-regulated protein	20	0.783 ± 0.086	0.855 ± 0.04	
48.41	96.8	P08462	GRPB_RAT	Submandibular gland secretory Glx-rich protein CB	33	1.868 ± 0.228		1.518 ± 0.125
16.69	62.4	P08010	GSTM2_RAT	Glutathione *S*-transferase Mu 2	8	1.615 ± 0.173		1.063 ± 0.27
15.1	51.7	O70351	HCD2_RAT	3-hydroxyacyl-CoA dehydrogenase Type-2	9	0.651 ± 0.042		
13.21	45.2	Q9WVK7	HCDH_RAT	Hydroxyacyl-coenzyme A dehydrogenase, mitochondrial	8	0.597 ± 0.017		0.782 ± 0.013
26.97	54.2	P63018	HSP7C_RAT	Heat shock cognate 71 kDa protein	12	1.369 ± 0.071		
18.97	40.3	Q63617	HYOU1_RAT	Hypoxia up-regulated protein 1	10		0.86 ± 0.032	
4.92	10.9	Q99NA5	IDH3A_RAT	Isocitrate dehydrogenase [NAD] subunit alpha, mitochondrial	4	0.442 ± 0.058		
24.36	49.1	P56574	IDHP_RAT	Isocitrate dehydrogenase [NADP], mitochondrial	14	0.742 ± 0.084	1.208 ± 0.081	
10.19	30.1	Q3KR86	IMMT_RAT	Mitochondrial inner membrane protein (Fragment)	5	0.611 ± 0.173		0.796 ± 0.004
35.05	61.5	P25809	KCRU_RAT	Creatine kinase U-type, mitochondrial	29	0.598 ± 0.14	1.178 ± 0.064	0.756 ± 0.044
105.3	92.7	P36375	KLK10_RAT	Glandular kallikrein-10	83	0.519 ± 0.085	0.993 ± 0.242	
41.11	93.1	P15950	KLK3_RAT	Glandular kallikrein-3, submandibular (fragment)	24	0.475 ± 0.051		
72.69	96.9	P36374	KLK6_RAT	Prostatic glandular kallikrein-6	55	0.692 ± 0.143	1.428 ± 0.037	1.116 ± 0.198
85.2	93.1	P07647	KLK9_RAT	Submandibular glandular kallikrein-9	71	0.598 ± 0.018	1.144 ± 0.028	
15.84	34.2	Q62902	LMAN1_RAT	Protein ERGIC-53	10	0.575 ± 0.02		
5.66	24.8	P97700	M2OM_RAT	Mitochondrial 2-oxoglutarate/malate carrier protein	3	0.533 ± 0.164		
13.71	29.7	Q02253	MMSA_RAT	Methylmalonate-semialdehyde dehydrogenase [acylating], mitochondrial	7	0.736 ± 0.063		
6.46	41.3	P16036	MPCP_RAT	Phosphate carrier protein, mitochondrial	3	0.51 ± 0.013	1.205 ± 0.033	0.785 ± 0.027
65.09	37.7	Q62812	MYH9_RAT	Myosin-9	45	0.773 ± 0.048	1.148 ± 0.097	1.183 ± 0.25
12.5	51.7	Q5BK63	NDUA9_RAT	NADH dehydrogenase [ubiquinone] 1 alpha subcomplex subunit 9, mitochondrial	8	0.617 ± 0.026		0.756 ± 0.031
14.8	36.2	Q66HF1	NDUS1_RAT	NADH-ubiquinone oxidoreductase 75 kDa subunit, mitochondrial	7	0.57 ± 0.168		0.725 ± 0.03
11.96	35.4	Q641Y2	NDUS2_RAT	NADH dehydrogenase [ubiquinone] iron-sulfur protein 2, mitochondrial	7	0.49 ± 0.054		
4.05	21.4	P19234	NDUV2_RAT	NADH dehydrogenase [ubiquinone] flavoprotein 2, mitochondrial	4	0.325 ± 0.021		
22.2	47.6	Q9JI85	NUCB2_RAT	Nucleobindin-2	13			0.723 ± 0.024
6.64	24.3	Q5XI78	ODO1_RAT	2-Oxoglutarate dehydrogenase, mitochondrial	4	0.649 ± 0.097		
16.73	53.2	P49432	ODPB_RAT	Pyruvate dehydrogenase E1 component subunit beta, mitochondrial	11	0.721 ± 0.101		

(continued)

Downloaded from http://jb.oxfordjournals.org/ at Pennsylvania State University on September 13, 2016

Table III. Continued

Total	% Cov	Accession #		Name	Peptides (95%)	D2M	C4M	D4M
4.58	14.7	P14882	PCCA_RAT	Propionyl-CoA carboxylase alpha chain, mitochondrial	2	0.53 ± 0.023		
9.84	34.9	P07633	PCCB_RAT	Propionyl-CoA carboxylase beta chain, mitochondrial	5	0.575 ± 0.044		
61.04	81.5	P04785	PDIA1_RAT	Protein disulphide-isomerase	36	1.272 ± 0.045	0.865 ± 0.039	1.02 ± 0.167
38.12	58	P11598	PDIA3_RAT	Protein disulphide-isomerase A3	24	1.32 ± 0.121	0.868 ± 0.026	
14.48	63.6	P31044	PEBP1_RAT	Phosphatidylethanolamine-binding protein 1	7	1.703 ± 0.319	1.129 ± 0.002	
5.12	29.4	P67779	PHB_RAT	Prohibitin	3	0.361 ± 0.004		
7.01	36.5	Q5XIH7	PHB2_RAT	Prohibitin-2	4	0.524 ± 0.187		
19.11	67.1	P10111	PPIA_RAT	Peptidyl-prolyl *cis–trans* isomerase A	16	1.613 ± 0.331		1.283 ± 0.105
4.49	27.9	P62963	PROF1_RAT	Profilin-1	3	1.875 ± 0.233		
5.08	52.9	P04550	PTMS_RAT	Parathymosin	2	2.005 ± 0.268		
6.27	12.1	P52873	PYC_RAT	Pyruvate carboxylase, mitochondrial	3	0.44 ± 0.087		
16.17	27.6	P53534	PYGB_RAT	Glycogen phosphorylase, brain form (Fragment)	12	1.75 ± 0.383	1.218 ± 0.028	
7.76	32.7	Q68FY0	QCR1_RAT	Cytochrome b-c1 complex subunit 1, mitochondrial	6	0.371 ± 0.008		
13.29	33	P32551	QCR2_RAT	Cytochrome b-c1 complex subunit 2, mitochondrial	10	0.45 ± 0.136		0.715 ± 0.001
10.83	44.9	Q5M9I5	QCR6_RAT	Cytochrome b-c1 complex subunit 6, mitochondrial	8	0.508 ± 0.176		
5.6	34.8	P62914	RL11_RAT	60S ribosomal protein L11	3	0.664 ± 0.086		
10.81	45.6	P61314	RL15_RAT	60S ribosomal protein L15	4	0.677 ± 0.056		0.696 ± 0.055
13.71	47.7	P21533	RL6_RAT	60S ribosomal protein L6	11	0.809 ± 0.024		
3.29	54.2	P62864	RS30_RAT	40S ribosomal protein S30	2			0.716 ± 0.076
7.78	40.7	P29314	RS9_RAT	40S ribosomal protein S9	4	0.694 ± 0.034		
16.81	71.5	P38983	RSSA_RAT	40S ribosomal protein SA	8	0.759 ± 0.016		
3.64	66.3	P05964	S10A6_RAT	Protein S100-A6	3	1.925 ± 0.229		2.15 ± 0.279
6.42	22	P10760	SAHH_RAT	Adenosylhomocysteinase	3		0.711 ± 0.035	
11.7	31.9	B2GV06	SCOT1_RAT	Succinyl-CoA:3-ketoacid-coenzyme A transferase 1, mitochondrial	7	0.623 ± 0.049		0.762 ± 0.065
21.5	75.3	P13432	SMR1_RAT	SMR1 protein	18	0.591 ± 0.03		
18.4	69.3	P18897	SMR2_RAT	SMR2 protein	8	1.718 ± 0.157		
22.14	39.8	Q66X93	SND1_RAT	Staphylococcal nuclease domain-containing protein 1	13	0.756 ± 0.02	0.825 ± 0.028	
33.79	25.6	P16086	SPTA2_RAT	Spectrin alpha chain, brain	16	1.238 ± 0.05		
3.33	25.7	Q7TPJ0	SSRA_RAT	Translocon-associated protein subunit alpha	4	0.463 ± 0.162		
27.41	48.1	Q6P9V9	TBA1B_RAT	Tubulin alpha-1B chain	19	1.454 ± 0.108		
18.71	54.7	P17764	THIL_RAT	Acetyl-CoA acetyltransferase, mitochondrial	12	0.718 ± 0.04	1.208 ± 0.073	
7.31	41.6	Q63584	TMEDA_RAT	Transmembrane emp24 domain-containing protein 10	4	0.539 ± 0.055		0.74 ± 0.054
4.4	19.7	P48500	TPIS_RAT	Triosephosphate isomerase	2	1.92 ± 0.138		
12.53	36.6	P04692	TPM1_RAT	Tropomyosin alpha-1 chain	7		1.407 ± 0.136	
11.62	24.4	P12346	TRFE_RAT	Serotransferrin	5	1.407 ± 0.129		
11.55	22.9	Q5U300	UBA1_RAT	Ubiquitin-like modifier-activating enzyme 1	7	1.495 ± 0.219		
4.14	36.1	P20788	UCRI_RAT	Cytochrome b-c1 complex subunit Rieske, mitochondrial	3	0.416 ± 0.155		

Ratios are presented as mean ± SD.

belong to processes that were down-regulated. From these, it is observable a clear down-regulation of the metabolic process and generation of precursor metabolites and energy proteins. From the processes found up-regulated, which corresponded to 37% of the proteins identified, the transport, cellular process and cell communication processes are worth of note, besides the metabolic process already mentioned in the down-regulated category. After 4 months of hyperglycemia, the majority of proteins (>60%) presented no variations, reflecting a tendency of adaptation to the chronic hyperglycemia. Nonetheless, within the up- and down-regulated processed, the distribution remained similar to the one observed in the C2M group. In general, it was noticed an up-regulation of annexins, calmodulin, sodium/potassium transporting ATPase subunits and SMG secretory Glx-rich protein CB associated with hyperglycemia, although these variations were attenuated with time (Fig. 3).

Downloaded from http://jb.oxfordjournals.org/ at Pennsylvania State University on September 13, 2016

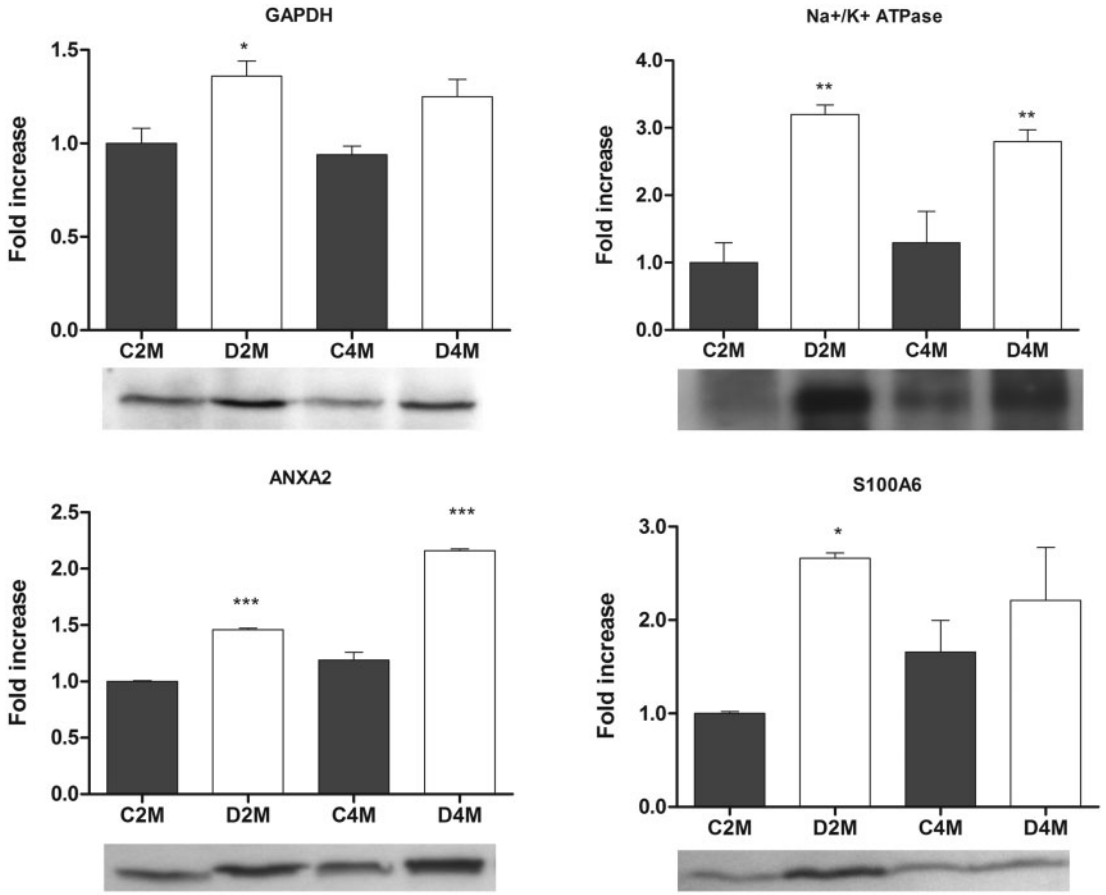

Fig. 2 Western blot analysis of GAPDH, alpha 1 sodium potassium ATPase, annexin A2 and protein S100A6 showing an up-regulation of these proteins in groups treated with STZ, confirming the tendency observed in iTRAQ quantification. A representative immunoblot image is presented below the histogram. Data are presented as mean ± SD. $*P<0.05$, $**P<0.01$, $***P<0.001$.

Table IV. Distribution of the genes corresponding to the proteins identified in the iTRAQ assay by GO Biological Process.

	D2M (189 genes)			D4M (90 genes)		
Biological process	↓	=	↑	↓	=	↑
Cell communication (GO:0007154)			4.8%		3.3%	3.3%
Cell cycle (GO:0007049)	3.2%		2.6%		2.2%	2.2%
Cellular component organization (GO:0016043)	0.5%	1.6%	1.6%		5.6%	
Cellular process (GO:0009987)	3.7%	1.6%	6.3%		10.0%	3.3%
Developmental process (GO:0032502)	2.6%	1.6%	3.2%		6.7%	2.2%
Generation of precursor metabolites and energy (GO:0006091)	12.2%			4.4%	5.6%	
Homeostatic process (GO:0042592)		0.5%	0.5%	1.1%		1.1%
Immune system process (GO:0002376)	0.5%	0.5%	1.6%		2.2%	1.1%
Metabolic process (GO:0008152)	22.8%	2.6%	8.5%	5.6%	15.6%	5.6%
Response to stimulus (GO:0050896)	0.5%	0.5%	1.1%		2.2%	
System process (GO:0003008)	0.5%		0.5%		1.1%	
Transport (GO:0006810)	6.9%	0.5%	6.3%	2.2%	8.9%	4.4%
Total	53.4%	9.5%	37.0%	13.3%	63.3%	23.3%

Each percentage was calculated by dividing the number of genes in each category by the total number of genes in the group.↓ down--regulated; = no variation; ↑ up-regulated.

Discussion

The influence of diabetes and hyperglycemia in the ultrastructure and protein activity of salivary glands has been demonstrated (*8*, *10*, *18*). However, a more in-depth proteomic analysis could provide important information regarding the intra-cellular changes that occur throughout a prolonged exposure to hyperglycemia.

STZ-induced destruction of pancreatic beta-cells has been extensively applied in the study of diabetes and hyperglycemia in animal models, including the study of its effects in salivary glands (*8*, *16*, *18*, *19*). Our goal was to apply a proteomic approach to SMG fractions, as major contributors for unstimulated saliva, and further disclose the molecular mechanisms responsible for the morphological alterations previously reported.

Downloaded from http://jb.oxfordjournals.org/ at Pennsylvania State University on September 13, 2016

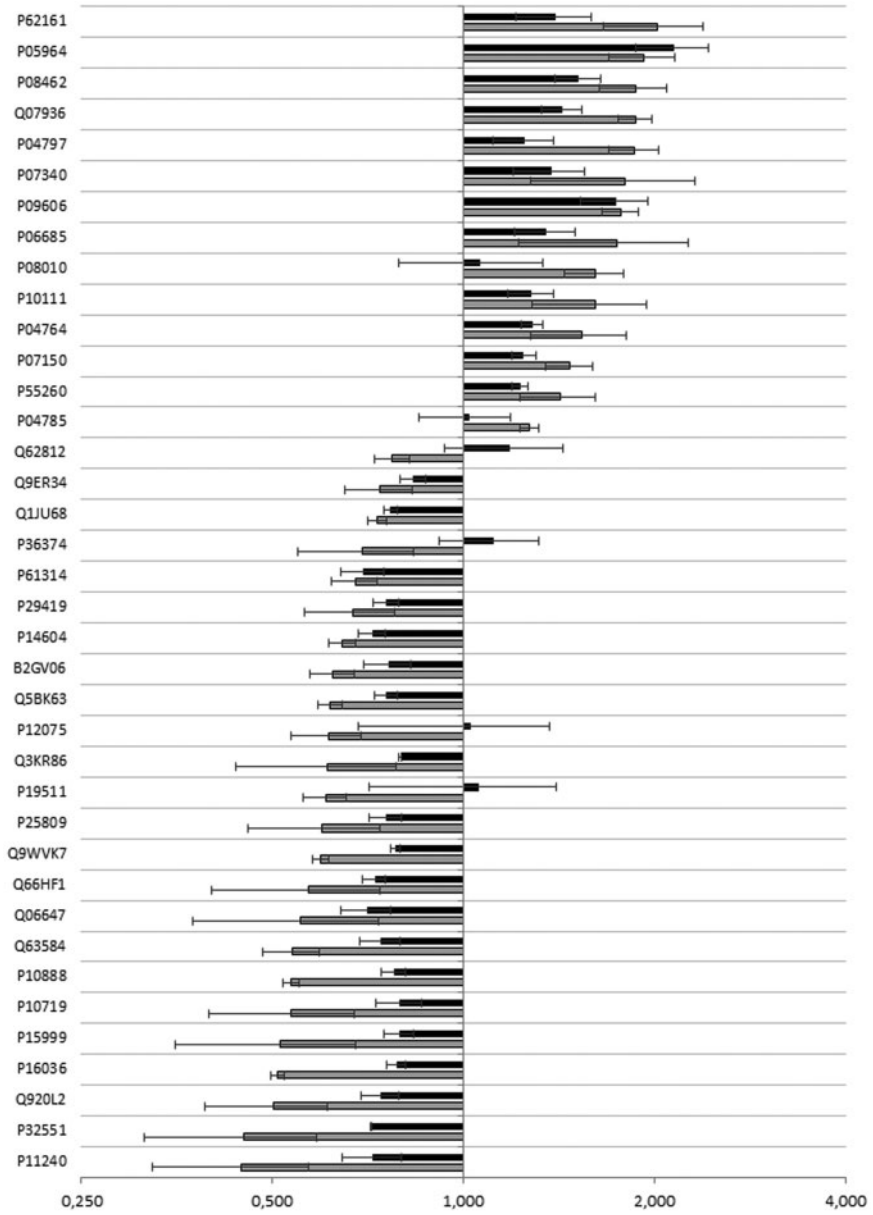

Fig. 3 Comparison of the variation values at two (grey bars) and four (black bars) months of hyperglycemia. It is observable a tendency to reduce the variation at 4 months, compared with the 2 months value. Proteins are identified by Uniprot ID on the left side. Data are presented as mean ± SD of the variation versus the C2M group.

We began by identifying the proteome constitution of our fractions. The presence of a high percentage of proteins classified as belonging to the GO biological processes of protein transport, cellular component organization, vesicle-mediated transport and exocytosis (Table II) clearly points towards enrichment in secretory granules and other vesicular structures, with some mitochondria contribution. The iTRAQ quantitative analysis provided an evaluation of the impact of STZ-induced diabetes in SMG and its evolution with the progressing of the disease.

Considering the ultrastructural changes reported for salivary glands in diabetes (*10*), it was not surprising to observe a down-regulation of the metabolic and energy production processes. However, the variations observed for proteins such as kallikreins and protein S100A6, for their role in inflammation and tissue regeneration, as well as annexins and clathrin, for their role in vesicular transport, are worth of a closer analysis.

Kallikreins play an important role in saliva production, namely in the activation of several proteins as proline-rich proteins (*27*) or matrix-metalloproteinases. Moreover, Chan *et al.* (*21*) have reported a decreased activity of kallikrein and kallikrein-like proteases in salivary glands of diabetic rats. Our sample was highly enriched in kallikreins and we describe the down-regulation of kallikreins 3, 6, 9 and 10 after 2 months of hyperglycemia (Table III). Kallikreins have been suggested to play a role in the maintenance of oral health either indirectly by proteolytic activation of proteins such as proline-rich protein

Downloaded from http://jb.oxfordjournals.org/ at Pennsylvania State University on September 13, 2016

(*27*) that act in the protection and repair of dental enamel against dental caries (*28*) or directly as mediators of vasodilatation in injured areas of the oral mucosa, allowing a more efficient defense and faster healing (*29*). It has also been suggested an involvement in cell survival and proliferation, as kinins bind G-coupled receptors B1 and B2 may activate the pro-survival PI3K-Akt pathway, and salivary glands express these receptors (*30*, *31*). Since histochemical studies reported the predominance of glandular kallikreins in the striated ducts and ductal cells of SMGs of primates (*32*) and rodents (*33*), the down-regulation observed herein may, in one hand, compromise the regeneration ability of the gland, and in the other hand be justified by higher susceptibility of ductal cells to STZ-induced diabetes, as reported by Anderson *et al.* (*10*). It is also worth noting the extremely pronounced up-regulation of protein S100A6 after 2 months of hyperglycemia (Fig. 2). This protein is a trigger for apoptosis through the activation of JNK, a member of the mitogen-activated kinases mostly involved in stress response (*34*, *35*), and its up-regulation clearly suggests that apoptotic events are linked to the observed loss of glandular mass and function.

As stated above, another family of proteins that stands out from the list of identified proteins was the annexins family. Indeed, from a total of seven entries for rat annexins in Uniprot, we have identified five of them. Annexins are calcium-binding proteins that were shown to be involved in intracellular trafficking and organization of vesicles (*36*, *37*). Some of the members of this family, such as annexin A1, have been associated with an anti-inflammatory effect (*38*). Our iTRAQ-based quantitative analysis shows an up-regulation of annexins in diabetic rats, this tendency was further confirmed by western blot analysis of annexin A2 (Fig. 2), as well as an up-regulation of clathrin light chain A (Table III and Fig. 2). Considering that diabetes is often associated with an increased inflammatory state, namely in the oral cavity, the up-regulation of these proteins should be expected. However, one cannot exclude that annexins may play a role in granule fusion, which is another well-known ultrastructural modification in salivary gland associated with diabetes (*8*).

Regarding the temporal effect of hyperglycemia on the proteome constitution, our results suggest an adaptation of the tissue, with the reduction of the variation values at 4 months, when compared with the 2 months animals, as can be depicted from Fig. 3. This pattern indicates the presence of two kind of response to the stress caused by hyperglycemia. At 2 months, we have an early phase response with highly marked variations of several proteins, mostly down-regulations, while at 4 months, the variations are attenuated in a clear sign of adaptation to the chronic hyperglycemia, which is also evidenced in the biological processes altered (Table IV).

In overall, our results provide interesting evidence of the biochemical events underlying the morphological alterations previously reported, namely the loss of gland mass through apoptosis and loss of regeneration ability. Also, we observe an adaptation of the gland to the hyperglycemic state, through a more intense variation of some proteins at 2 months, which tend to normalize over time. As such, these results not only contribute to the comprehension of the morphological alterations but also open new pathways for the complete unravelling of the molecular mechanisms responsible for the link between diabetes mellitus and oral health decline.

Supplementary Data

Supplementary Data are available at *JB* Online.

Acknowledgements

The authors acknowledge the technical support of Celeste Resende in animal care.

Funding

This work was supported by the Foundation for Science and Technology of the Portuguese Ministry of Education and Science [PTDC/QUI/72903/2006 and PEst-C/QUI/UI0062/2011, PhD fellowship SFRH/BD/46829/2008 to RMPA].

Conflict of interest

None declared.

References

1. Wild, S., Roglic, G., Green, A., Sicree, R., and King, H. (2004) Global prevalence of diabetes: estimates for the year 2000 and projections for 2030. *Diabetes Care* **27**, 1047–1053
2. Narayan, K.M.V., Zhang, P., Kanaya, A.M., Williams, D.E., Engelgau, M.M., Imperatore, G., and Ramachandran, A. (2006) Diabetes: the pandemic and potential solutions in *Disease Control Priorities in Developing Countries* (Jamison, D.T., Breman, J.G., Measham, A.R., Alleyne, G., Claeson, M., Evans, D.B., Jha, P., Mills, A., and Musgrove, P., eds.), pp. 591–603, Washington, DC
3. Lakschevitz, F., Aboodi, G., Tenenbaum, H., and Glogauer, M. (2011) Diabetes and periodontal diseases: interplay and links. *Curr. Diabetes Rev.* **7**, 433–439
4. Moore, P.A., Guggenheimer, J., Etzel, K.R., Weyant, R.J., and Orchard, T. (2001) Type 1 diabetes mellitus, xerostomia, and salivary flow rates. *Oral Surg. Oral Med. Oral Pathol. Oral Radiol. Endod.* **92**, 281–291
5. Sreebny, L.M., Yu, A., Green, A., and Valdini, A. (1992) Xerostomia in diabetes mellitus. *Diabetes Care* **15**, 900–904
6. Navazesh, M. (1993) Methods for collecting saliva. *Ann. N.Y. Acad. Sci.* **694**, 72–77
7. Szkudelski, T. (2001) The mechanism of alloxan and streptozotocin action in B cells of the rat pancreas. *Physiol. Res.* **50**, 537–546
8. Cutler, L.S., Pinney, H.E., Christian, C., and Russotto, S.B. (1979) Ultrastructural studies of the rat submandibular gland in streptozotocin induced diabetes mellitus. *Virchows Arch. A Pathol. Anat. Hist.* **382**, 301–311
9. Anderson, L.C., Garrett, J.R., Suleiman, A.H., Proctor, G.B., Chan, K.M., and Hartley, R. (1993) In vivo secretory responses of submandibular glands in streptozotocin-diabetic rats to sympathetic and parasympathetic nerve stimulation. *Cell Tissue Res.* **274**, 559–566

Downloaded from http://jb.oxfordjournals.org/ at Pennsylvania State University on September 13, 2016

10. Anderson, L.C., Suleiman, A.H., and Garrett, J.R. (1994) Morphological effects of diabetes on the granular ducts and acini of the rat submandibular gland. *Microsc. Res.Tech.* **27**, 61–70
11. Walz, A., Stuhler, K., Wattenberg, A., Hawranke, E., Meyer, H.E., Schmalz, G., Bluggel, M., and Ruhl, S. (2006) Proteome analysis of glandular parotid and submandibular-sublingual saliva in comparison to whole human saliva by two-dimensional gel electrophoresis. *Proteomics* **6**, 1631–1639
12. Caseiro, A., Vitorino, R., Barros, A.S., Ferreira, R., Calheiros-Lobo, M.J., Carvalho, D., Duarte, J.A., and Amado, F. (2012) Salivary peptidome in type 1 diabetes mellitus. *Biomed. Chromatogr.* **26**, 571–582
13. Vitorino, R., Alves, R., Barros, A., Caseiro, A., Ferreira, R., Lobo, M.C., Bastos, A., Duarte, J., Carvalho, D., Santos, L.L., and Amado, F.L. (2010) Finding new post-translational modifications in salivary proline-rich proteins. *Proteomics* **10**, 3732–3742
14. Vitorino, R., Lobo, M.J., Ferrer-Correira, A.J., Dubin, J.R., Tomer, K.B., Domingues, P.M., and Amado, F.M. (2004) Identification of human whole saliva protein components using proteomics. *Proteomics* **4**, 1109–1115
15. Denny, P., Hagen, F.K., Hardt, M., Liao, L., Yan, W., Arellanno, M., Bassilian, S., Bedi, G.S., Boontheung, P., Cociorva, D., Delahunty, C.M., Denny, T., Dunsmore, J., Faull, K.F., Gilligan, J., Gonzalez-Begne, M., Halgand, F., Hall, S.C., Han, X., Henson, B., Hewel, J., Hu, S., Jeffrey, S., Jiang, J., Loo, J.A., Ogorzalek Loo, R.R., Malamud, D., Melvin, J.E., Miroshnychenko, O., Navazesh, M., Niles, R., Park, S.K., Prakobphol, A., Ramachandran, P., Richert, M., Robinson, S., Sondej, M., Souda, P., Sullivan, M.A., Takashima, J., Than, S., Wang, J., Whitelegge, J.P., Witkowska, H.E., Wolinsky, L., Xie, Y., Xu, T., Yu, W., Ytterberg, J., Wong, D.T., Yates, J.R. 3rd, and Fisher, S.J. (2008) The proteomes of human parotid and submandibular/sublingual gland salivas collected as the ductal secretions. *J. Proteome Res.* **7**, 1994–2006
16. Ibuki, F.K., Simoes, A., and Nogueira, F.N. (2010) Antioxidant enzymatic defense in salivary glands of streptozotocin-induced diabetic rats: a temporal study. *Cell Biochem. Funct.* **28**, 503–508
17. Anderson, L.C. and Shapiro, B.L. (1979) The effect of alloxan diabetes and insulin in vivo on peroxidase activity in the rat submandibular gland. *Arch. Oral Biol.* **24**, 343–345
18. Mednieks, M.I., Szczepanski, A., Clark, B., and Hand, A.R. (2009) Protein expression in salivary glands of rats with streptozotocin diabetes. *Int. J. Exp. Pathol.* **90**, 412–422
19. Szczepanski, A., Mednieks, M.I., and Hand, A.R. (1998) Expression and distribution of parotid secretory proteins in experimental diabetes. *Eur. J. Morphol.* **36 (Suppl.)**, 240–246
20. Kasayama, S., Ohba, Y., and Oka, T. (1989) Epidermal growth factor deficiency associated with diabetes mellitus. *Proc. Natl Acad. Sci. USA* **86**, 7644–7648
21. Chan, K.M., Chao, J., Proctor, G.B., Garrett, J.R., Shori, D.K., and Anderson, L.C. (1993) Tissue kallikrein and tonin levels in submandibular glands of STZ-induced diabetic rats and the effects of insulin. *Diabetes* **42**, 113–117
22. Feinstein, H. and Schramm, M. (1970) Energy production in rat parotid gland. Relation to enzyme secretion and effects of calcium. *Eur. J. Biochem.* **13**, 158–163
23. Manadas, B., English, J.A., Wynne, K.J., Cotter, D.R., and Dunn, M.J. (2009) Comparative analysis of OFFGel, strong cation exchange with pH gradient, and RP at high pH for first-dimensional separation of peptides from a membrane-enriched protein fraction. *Proteomics* **9**, 5194–5198
24. Vitorino, R., Barros, A., Caseiro, A., Domingues, P., Duarte, J., and Amado, F. (2009) Towards defining the whole salivary peptidome. *Proteom Clin. Appl.* **3**, 528–540
25. Gan, C.S., Chong, P.K., Pham, T.K., and Wright, P.C. (2007) Technical, experimental, and biological variations in isobaric tags for relative and absolute quantitation (iTRAQ). *J. Proteome Res.* **6**, 821–827
26. Laemmli, U.K. (1970) Cleavage of structural proteins during the assembly of the head of bacteriophage T4. *Nature* **227**, 680–685
27. Wong, R.S., Madapallimattam, G., and Bennick, A. (1983) The role of glandular kallikrein in the formation of a salivary proline-rich protein A by cleavage of a single bond in salivary protein C. *Biochem. J.* **211**, 35–44
28. Levine, M. (2011) Susceptibility to dental caries and the salivary proline-rich proteins. *Int. J. Dent.* **2011**, 953412
29. Fábián, T.K., Fejérdy, P., and Csermely, P. (2008) Saliva in health and disease (chemical biology of) *Wiley Encyclopedia of Chemical Biology* (Begley, T.P., ed.), pp. 1–9, John Wiley and Sons, Inc
30. Dlamini, Z. and Bhoola, K.D. (2005) Upregulation of tissue kallikrein, kinin B1 receptor, and kinin B2 receptor in mast and giant cells infiltrating oesophageal squamous cell carcinoma. *J. Clin. Pathol.* **58**, 915–922
31. Bader, M. (2009) Kallikrein-kinin system in neovascularization. *Arterioscler. Thromb. Vasc. Biol.* **29**, 617–619
32. Yahiro, J. and Miyoshi, S. (1996) Immunohistochemical localization of kallikrein in salivary glands of the Japanese monkey, Macaca fuscata. *Arch. Oral Biol.* **41**, 225–228
33. Garrett, J.R., Smith, R.E., Kidd, A., Kyriacou, K., and Grabske, R.J. (1982) Kallikrein-like activity in salivary glands using a new tripeptide substrate, including preliminary secretory studies and observations on mast cells. *Histochem. J.* **14**, 967–979
34. Leclerc, E., Fritz, G., Weibel, M., Heizmann, C.W., and Galichet, A. (2007) S100B and S100A6 differentially modulate cell survival by interacting with distinct RAGE (receptor for advanced glycation end products) immunoglobulin domains. *J. Biol. Chem.* **282**, 31317–31331
35. Schaeffer, H.J. and Weber, M.J. (1999) Mitogen-activated protein kinases: specific messages from ubiquitous messengers. *Mol. Cell. Biol.* **19**, 2435–2444
36. Gerke, V., Creutz, C.E., and Moss, S.E. (2005) Annexins: linking Ca2+ signalling to membrane dynamics. *Nat. Rev. Mol. Cell Biol.* **6**, 449–461
37. Donnelly, S.R. and Moss, S.E. (1997) Annexins in the secretory pathway. *Cell. Mol. Life Sci.* **53**, 533–538
38. Lim, L.H. and Pervaiz, S. (2007) Annexin 1: the new face of an old molecule. *FASEB J.* **21**, 968–975

Downloaded from http://jb.oxfordjournals.org/ at Pennsylvania State University on September 13, 2016